19th International Computer Science and Engineering Conference (ICSEC)
Chiang Mai, Thailand, 23-26 November, 2015

Plant Cover Detection from Visible Satellite Imagery

Arcchaporn Choukuljaratsiri
School of Management
National Taiwan University of Science and Technology
Taipei City, Taiwan
M10421814@mail.ntust.edu.tw

Pimwadee Chaovalit and Suporn Pongnumkul
Computational Process Analytics Research Laboratory
National Electronics and Computer Technology Center
Pathum Thani, Thailand
pimwadee.chaovalit@nectec.or.th,
suporn.pongnumkul@nectec.or.th

Abstract— **This paper explores green field detection methods for visible satellite images by applying well-known combination of vegetative index (COM), and developing two methods that are enhanced versions of COM to increase detection accuracies. An experiment was conducted on visible satellite images of 6 locations and 4 zoom levels obtained through Google Map API. The three methods were implemented to compare the detection accuracies. Results show that the proposed methods improved detection accuracies (computed using F-Measures) of the test image set.**

Keywords—Remote-Sensing; Image Processing; Vegetative Index;

I. INTRODUCTION

Like in many other developing countries, agriculture is the main occupation in Thailand. Appropriate management of agricultural information is, therefore, a key for the country's development. One important information is the accurate map of farmlands, which is crucial for evaluating the country's state of agriculture, natural resource, land use and planning, mapping/surveying and infrastructure planning.

There exist many methods for farmland mapping, which include field survey and farmland detection from terrestrial images, aerial images, and satellite images. This paper explores algorithms for extracting farm areas from satellite images. While image-processing methods to detect green plant cover area from satellite images have been implemented in the field of remote sensing for many years, such methods normally include non-visible light spectrum (e.g. infrared). The methods that use only visible light images (red, green, blue spectrum) have not been explored much in the literature. With the increasing availability of satellite image data from commercial online map providers (e.g. Google maps, Yahoo maps), satellite image data with only visible light are available for viewing for any users with internet access. Therefore, detection methods that use only visible light images could be beneficial for areas where no other data is available.

To detect areas within a satellite image where plants are grown, this paper adopts vegetation indices (COM), which was proposed by Guijarro et al. [1] as a baseline method. COM has been used to detect agriculture areas in terrestrial images. Two more methods are proposed to solve detection errors found during initial experiments. The first method, *COM & Excess Red*, aims to solve detection errors where brown leaves were not detected as plant areas. The second method, *COM, Excess Red & Rule filter*, aims to reduce detection errors where the entire image consisting of no plant area were detected as plant area.

To evaluate the proposed methods, an experiment was conducted with input images in 3 spectral-bands (blue, green, red) at high resolution from Google's static map API [2]. Six areas were selected to represent six image characteristics and detection accuracies are presented.

II. RELATED WORK

A. Farmland Detection from Aerial or Satellite Images

Rongqun and Daolin [3] classified land use from satellite images by performing three types of analyses: spectral analysis, texture features analysis, and shape features analysis. Using reflectance values of four spectral bands (blue, green, red, and near infrared) along with texture and shape features (e.g. histograms, entropy, contrast, etc.), they classified objects on land into various types: building, road, forestland, farmland, standard water body, nonstandard water body, and shadow. Forestland and farmland have almost identical reflectance values in the visible band, but reflectance values in the near infrared band of farmland are more than those of forestland. Rules for classifying forestland and farmland were obtained: a) Ratio Vegetation Index (RVI) >1.7 and b) band4 (near infrared) = 200-600. An experiment on 600 images showed that accuracies of farmland and forestland extraction were both more than 90%.

Than et al. [4] built a theoretical model to detect rice field areas and their growth stages based on ERS-1 experimental data. In doing so, a technique called radar backscattering coefficient was used. The authors observed that radar backscattering coefficients can be used to interpret experimental data. Results from the obtained theoretical model appeared to align with the experimental data.

Sarkar et al. [5] used a Markov Random Field (MRF) framework in their segmentation of multispectral images for land cover classification. An MRF-based segmentation scheme was chosen to perform over initially oversegmented images and aimed to capture both textural and tonal features of multi band images. The authors applied a minimization on the MRF's energy function to merge previously segmented nodes within images. The approach was evaluated quantitatively for the images' clusters and compared with maximum likelihood approach.

978-1-4673-7825-3/15/$31.00 ©2015 IEEE

Almeer [6] proposed extracting vegetation areas from satellite images using Back Propagation Neural Network that worked with images of poor color quality. The method was aimed largely to work with desert areas of Qatar. The author first transformed images in RGB color space to HSV color space in order to cancel the effects of brightness and illumination within the images. Binary classified images of vegetation areas from desert, urban, and road street zones were illustrated. The method was useful in classifying satellite images. However, certain cases were challenging and not very effective. The method was still confused when discriminating between urban and desert areas and between desert and vegetation areas.

Torres-Sánchez et al. [7] used six visible spectral indices (CIVE, ExG, ExGR, Woebbecke Index, NGRDI, and VEG) to calculate vegetation fraction (VF) mapping from high-resolution aerial images taken from the UAV (Unmanned Aerial Vehicle) over a wheat field. Vegetation fraction is the fraction of occupation of vegetation canopy in a given ground area in vertical projection [8]. Among the six indices and two combinations of these indices, the ExG and VEG indices yielded the highest accuracy on vegetation mapping based on their experiment on a wheat field.

B. Farmland Detection from Terrestrial Images

Wanlor and Phiphobmongkol [9] applied an image processing technique on captured images of street views for rice field detection. They performed segmentation on images and then extracted image features, such as texture, color, and position, within each segment. An artificial neural network was constructed to determine whether the input features represented green plant level in each segment. Finally, a heuristic function using a ratio of green segment connection was applied to classify if the whole image was rice field. The more connected the segment, the more likely it was a rice field. The experiment produced a 99% accuracy for rice field detection and a 96% accuracy for non-rice field detection.

Guerrero et al. [10] developed a real-time automatic expert system to detect crop row in maize field from images taken by agricultural vehicles. The system is composed of two main functions: image segmentation and crop row estimation. For image segmentation, they adopted the combination of vegetation indices (COM) which was proposed by Guijarro et al. [1] to separate green plants (i.e., crop and weed) from other components (e.g. soil) within the image. For crop row estimation, the binary segmentation of green patches was input for tracing and correcting expected crop lines using the knowledge of crop rows and camera geometry.

Montalvo et al. [11] designed an advanced crop identification system where crops masked from dust/soil could be identified. Since crop identification systems usually classify image sections of crop rows based on their greenness level, the authors included excess red index (ExGR) as an extra step on top of using the combination of vegetation indices (COM) to detect plants that lost their greenness after partly covered by soil dust or after treatment along with green plants.

III. METHODOLOGY

Input images used in this paper are in RGB color space. The algorithm we use here are divided into 3 methods.

A. Method1 – Combination of vegetation indices (COM)

Vegetation Indices (VIs) are combinations of surface reflectance at two or more wavelengths designed to highlight a particular property of vegetation [12]. In this work, only visible VIs were applied.

Guijarro et al. [1] proposed a combination of four vegetation indices, ExG, ExGR, CIVE, and VEG, to determinate greenness in images. This method has been previously used to discriminate the plant area from both high-resolution aerial [7] and terrestrial [10][11] field images.

COM was selected for this work because of the algorithm's performance and simplicity. The COM algorithm was explained in Guijarro et al. [1]. We select to set the same parameters as specified by Guijarro et al. [1].

The result of COM algorithm is quantized into 256 gray levels, and Otsu's Threshold [13] method is applied to binarize the image. The generated result is the binary image which contains white pixels as green plant area and black pixels as others. Finally, dilations are applied to remove noise from the algorithm. The dilation settings and results are explained in the experiment section.

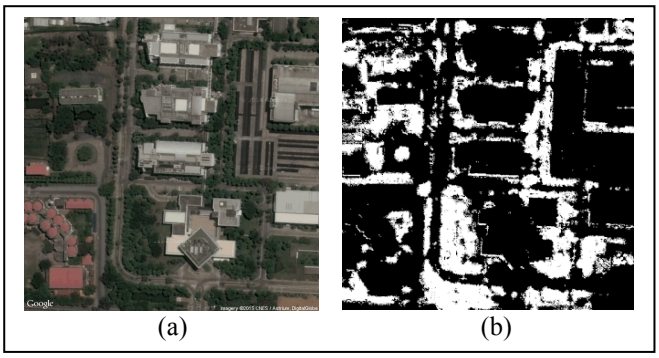

Fig. 1. Example of a COM convert;
(a) Original RGB Image, (b) COM Image

B. Method2 – COM & Excess Red

From Method1, a problem was found that some plant cover, which has brown leaves, possibly due to drying stage, was not detected as plant areas. Fig. 2 shows an example. Method2 is therefore aimed at reducing such detection errors.

This method utilizes the concept of [11] to extract data twice. The first round is to separate green leaf plant area by extracting COM value like Method1. The second round is to separate brown leaf areas from the left part by extracting Excess Red value from equation (6) to focus on red band intensity. Finally, we include white pixels area from both steps, optionally called "Logical OR" in image processing, into the final binary image result. The flowchart is shown in Fig. 3.

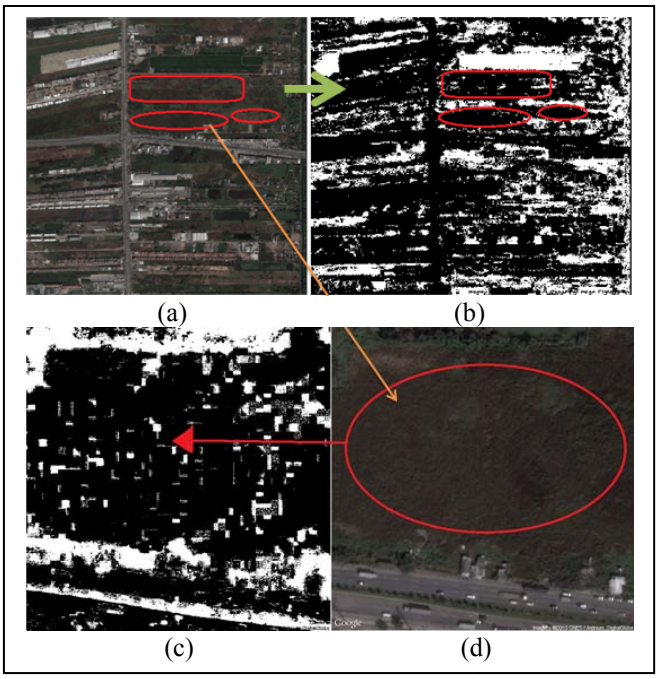

Fig. 2. Example of a brown leaf image;
(a)Original RGB Image, (b)COM Convert Image,
(c) Zoom in Com Image, (d) Zoom in RGB Image

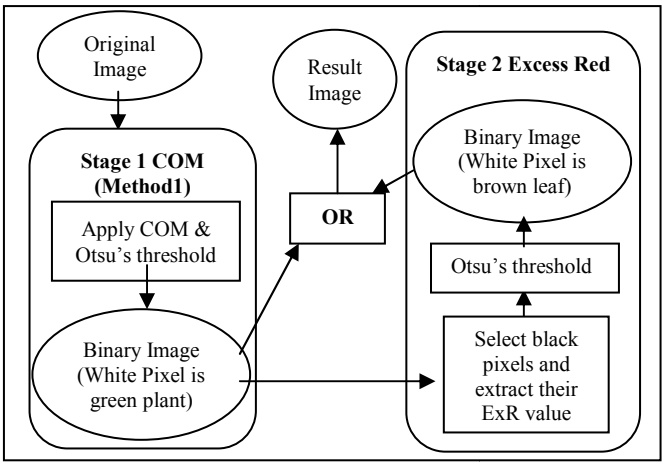

Fig. 3. Flowchart of Method2

C. *Method3 – COM, ExcessRed & Rule filter*

Method3 is proposed to solve the problems found during experiment from previous methods. First, images with little or no plant, e.g., town or desert, were incorrectly detected as all plant area. Another problem is that Method2 includes parts of bare soil area as white pixel because of its brown color. From our experiment, it is deducted that plant leaves only show obvious green or dark brown color. So the normalized and ratio index values from COM are simply applied for rule-based filter. The flowchart of rule-based filter is shown in Fig. 4.

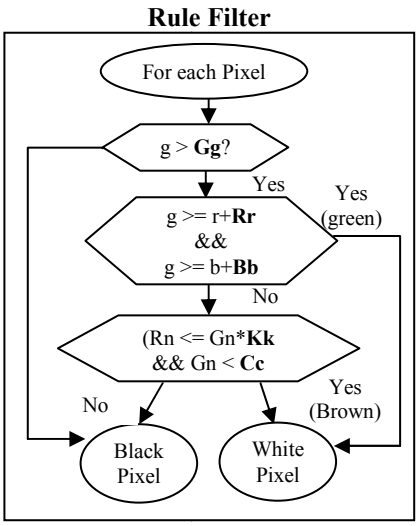

Fig. 4. Flowchart of rule-based filter used in Method3

The detail of rule-based filter is described as follows. First, a pixel has the possibility of being plant field only if its green intensity ratio (g) is more than Gg value. Second, a pixel represents the obvious green leaf area if g is more than the red intensity ratio (r) for Rr, and it is not the blue ocean if g is more than the blue intensity ratio (b) for Bb. Third, a pixel might represent the brown leaf area if the normalized value of red (R_n) is more than the normalized green (G_n), but not exceed G_n*Kk. And G_n is less than Cc.

Overall, the pixel should represent plant field if the first rule is true, and the second rule or third rule is true. In this work, each parameter is set as follows: $Gg = 0.32$, $Rr = 0.05$, $Bb = 0.013$, $Kk = 1.2$, and $Cc = 0.275$.

However, this rule should be applied only if the result images obtained from Method2 give detected green area much more than real expectation. So it is defined that if the two output images, from Method2 and rule filter, have matching pixels less than 50% of overall area, then the final result would be created from combining Method2 image with rule filter image by "Logical AND". In other words, the final binary image shows white pixels only at the positions where images from Method2 and rule filter also have white pixels. Otherwise, we use Method2 image as the output result image.

IV. Experiment

A. *Data Source*

We conducted an experiment on RGB satellite images obtained via Google map API [2] from 6 different locations. Each location was chosen to represent different land cover types as described in TABLE I. Sample images are shown in Fig. 5.

At each location, we collected images from 4 zoom levels, yielding a total of 24 images for our experiments. Equation (1) below explains how to determine pixel coordinates at a given zoom level from the world map [14]. The size for each image was 640 x 640 pixels.

$$pixelCoordinate = worldCoordinate * 2^{zoomLevel} \quad (1)$$

The selected zoom levels ranged from level 15 to level 18, because we considered that they are a suitable range for analyzing visible band information. Further zoomed-in images would show potentially noisy object textures or shadows. Further zoomed-out images would give high variance information in the same boundary.

TABLE I. LOCATION OF IMAGE SET

Location	Coordinate	Image Description
GreenField	15.4662081, 103.689594	All natural green field, mostly rice paddy
Island	11.7663482, 99.809409	A small island in blue ocean
MixedArea1	14.0777859, 100.6013131	Buildings connected with green field
MixedArea2	13.7549603, 100.747441	Partly brown-leaf field near buildings & factory sites
Airport	13.6939181, 100.7515523	Airport with small portions of green bushes
Forest	14.4066321, 101.3936871	All dense green forest

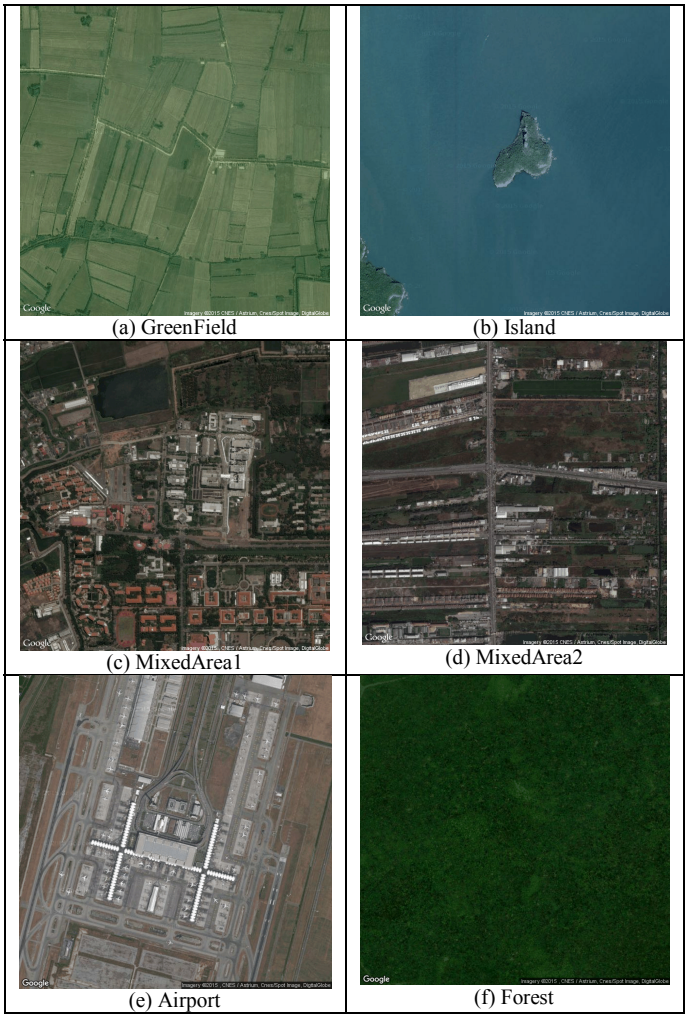

(a) GreenField (b) Island (c) MixedArea1 (d) MixedArea2 (e) Airport (f) Forest

Fig. 5. Sample input images at zoom level 16

B. Experiment Setup

We implemented image processing methods in Emgu CV, a cross-platform .Net wrapper to the OpenCV image processing library [15], on C#.Net. All 3 methods were applied with each input image. As a result, binary output images were generated. White pixels in the binary images represented green areas, whereas black pixels represented non-green areas. Dilation method was used to connect small gaps between white regions. Dilation mechanism was done by passing the kernel slide through the image (as in 2D convolution). A pixel in the original image, either white or black, would be considered white if at least one pixel under the kernel was white. Dilation increased white regions in the image or size of foreground object increased [16]. The dilation method of EmguCV implemented in this experiment can be repeated with the kernel size of 3x3 rectangular [17].

C. Evaluation Approach

We evaluated the methods presented in this paper by comparing green detection obtained from the methods with ground truth. Ground truth was constructed for each image as follows. Each input image was segmented into 30 x 30 pixels. Each segment was considered and marked manually for green field using a simple guideline. If green pixels were more than 60%, between 40-60%, and less than 40% of segmented area, the segment would be marked as true (green field), unsure, and false (non-green field), respectively. Fig. 6 illustrates markings of segments in an input image for all cases.

For green detection, we considered the proportion of white pixels (green area) within each segment of binary output images. If the number of white pixels exceeded 75% of total number of pixels, this segment was marked as green field. Accuracy numbers presented in this paper were calculated as F-measure. F-measure, defined as a harmonic mean of precision and recall, was selected for its balanced judgement on both precision and recall measures.

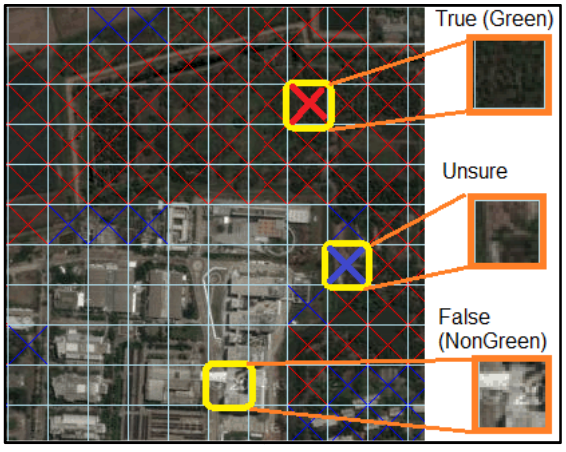

Fig. 6. Sample of input segment markings

D. Results

Dilation Effect

First, we experimented with dilation and the number of dilation iterations. Dilation was applied on Method1's binary output images. Binary pixels representing green area from output images could be disjoint. However, farmland usually is a patch of connected piece of land. Dilation was expected to connect detected green areas which were previously divided. Dilation iterations were varied from none to three times. TABLE II. summarizes green detection accuracy of Method 1 without dilation (dilation iteration is 0) and with dilation (dilation iteration ranging from 1 to 3). Accuracy percentages were averaged from results from all four zoom levels for each image location.

TABLE II. DILATION EFFECTS OF METHOD1

Location	Dilation 0	Dilation 1	Dilation 2	Dilation 3
GreenField	15.38	29.57	41.72	51.33
Island	15.79	18.79	18.86	19.08
MixedArea1	43.78	74.63	82.49	79.88
MixedArea2	23.46	50.87	64.95	73.54
Airport	4.25	39.54	39.85	32.49
Forest	0.12	95.16	99.66	99.83

From TABLE II. the accuracy generally increased with dilation iterations, with the exception of dilation 3 for MixedArea1 and Airport. We made a decision to investigate further into dilation 2 for our next experiment, as it seemed to give the most balanced result for this image set.

Comparison of All 3 Methods

All set of images were detected for green field area by all 3 methods with dilation iteration of 2. Average accuracies of zoom level 15-18 from all images are shown in TABLE III.

TABLE III. COMPARISONS OF ALL 3 METHODS

Location	Method1	Method2	Method3
GreenField	41.72	95.78	95.19
Island	18.86	19.05	71.90
MixedArea1	82.49	50.78	73.28
MixedArea2	64.95	81.23	90.85
Airport	39.85	7.04	52.55
Forest	99.66	100	100

From TABLE III., Method3 gave the best accuracy for Island, MixedArea2, and Airport image sets. For Island and MixedArea2 image sets, Method2 improved on accuracy from Method1 and Method3 improved on accuracy from Method 2. Accuracy result for the Airport Image is relatively low because most dark shadow was detected as green field.

As for GreenField, Method1 gave 41.72% accuracy, possibly because the detection method was based on combining ratio index value of RGB color range on Otsu's Threshold which assume that the image contains two classes of pixels following bi-modal histogram.

Since GreenField was primarily green, the discrimination of color range within the same image was not obvious. However, accuracy results for the GreenField image set from Method2 and Method3 gave satisfying results of over 95%. It is worth noting that Methods 2 and 3 for the MixedArea1 image set did not improve accuracy results. Method3's detection accuracy increased from that of Method2 due to an adjustment on correctly detecting non-green portion of the image. However, Method1 remained the technique giving the highest accuracy for the Mix edArea1 image set.

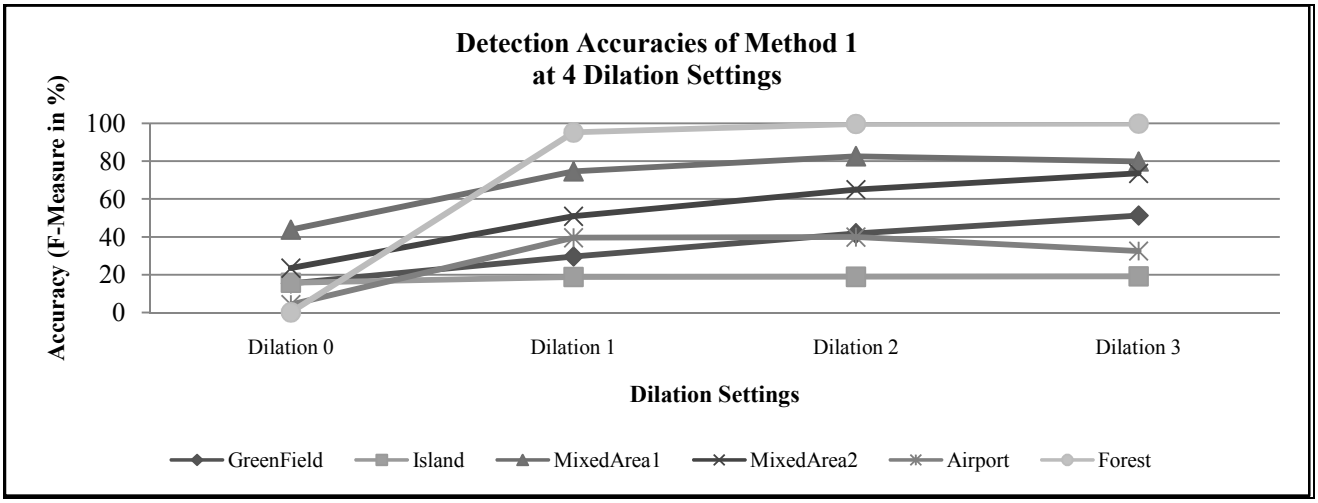

Fig 7. Dilation effects on detection accuracy for Method1

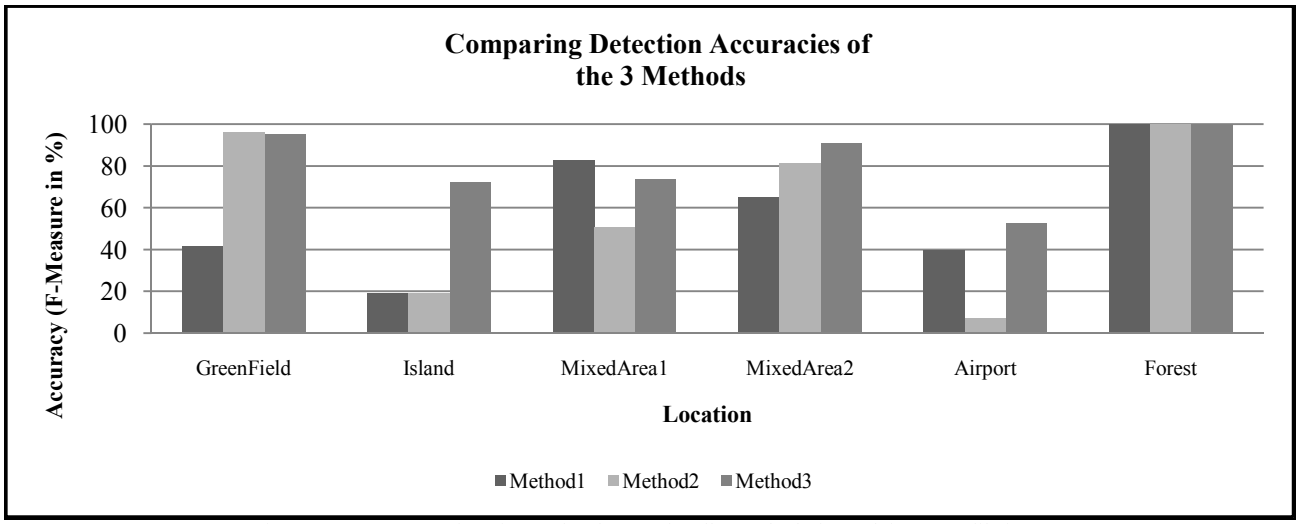

Fig. 8. Average accuracies of zoom level 15-18 for all 3 methods for each image at dilation 2

V. CONCLUSION

This paper applied the conventional COM extraction method (Method1) to satellite images to detect green plant areas and proposed two methods which enhanced COM to improve detection accuracy in cases where brown leaves were not detected as plant areas (Method2) and for images of an island surrounded by blue ocean (Method3). For the six selected areas in our experiments, Method1 acheived accuracy between 18.86-99.66%, while Method2 achieved accuracy between 7.04-100% and Method3 achieved accuracy between 52.55-100%. The results show that our proposed methods are promising to detect green plants from satellite images with RGB color space for a variety of area types.

REFERENCES

[1] M. Guijarro, G. Pajares, I. Riomoros, P.J. Herrera, X.P. Burgos-Artizzu, and A. Ribeiro, "Automatic segmentation of relevant textures in agricultural images," Computers and Electronics in Agriculture, vol. 75, Issue 1, pp. 75–83, January 2011.

[2] Google, Static Maps API, https://developers.google.com/maps/documentation/staticmaps/, accessed Jul 19th 2015.

[3] R. Zhang and D. Zhu, "Study of land cover classification based on knowledge rules using high-resolution remote sensing images," Expert Systems with Application, vol. 38, issue 4, pp. 3647-3652, April 2011.

[4] T. L. Toan, F. Ribbes, L.-F. Wang, N. Floury, K.-H. Ding, J. A. Kong, M. Fujita, and T. Kurosu, "Rice crop mapping and monitoring using ERS-1 data based on experiment and modeling Rrsults," IEEE Transactions on Geoscience and Remote Sensing, vol. 35, No. 1, pp. 41-56, January 1997.

[5] A. Sarkar, M. K. Biswas, B. Kartikeyan, V. Kumar, K. L. Majumder, and D. K. Pal, "A MRF model-based segmentation approach to classification for multispectral imagery," IEEE Transactions on Geoscience and Remote Sensing, vol. 40, no. 5, pp. 1102 - 1113, May 2002.

[6] M.H. Almeer, "Vegetation extraction from free Google Earth images of deserts using a robust BPNN approach in HSV space," International Journal of Advanced Research in Computer and Communication Engineering, vol. 2, Issue 5, May 2012.

[7] J. Torres-Sánchez, J.M. Peña, A.I. de Castro, F. López-Granados, "Multi-temporal mapping of the vegetation fraction in early-season wheat fields using images from UAV," Computers and Electronics in Agriculture, vol. 103, pp. 104-113, April 2014.

[8] Open Government Data (OGD) Platform India, Vegetation Fraction (VF), https://data.gov.in/keywords/vegetation-fraction-vf/, accessed Jul 20th 2015.

[9] C. Wanlor and S. Phiphobmongkol, "Rice field detection from terrestrial images," International Workshop on Advanced Image Technology, Bangkok, Thailand, January 6-8, 2014.

[10] J.M. Guerrero, M.Guijarro, M. Montalvo, J. Romeo, L. Emmi, A. Ribeiro, and G. Pajares, "Automatic expert system based on images for accuracy crop row detection in maize fields," Expert Systems with Applications, vol. 40, Issue 2, pp. 656 - 664, February 2013.

[11] M. Montalvo, J.M. Guerrero, J. Romeo, L. Emmi, M. Guijarro, and G. Pajares, "Automatic expert system for weeds/crops identification in images from maize field," Expert Systems with Application, vol. 40, Issue 1, pp. 75-82, January 2013.

[12] EXELIS, Vegetation Indices, http://www.exelisvis.com/docs/VegetationIndices.html/, accessed Jul 20th 2015.

[13] OpenCV-Python Tutorials, "Otsu's Binaraization", http://docs.opencv.org/master/d7/d4d/tutorial_py_thresholding.html, accessed Jul 29th 2015

[14] Google Maps JavaScript API, Pixel Coordinates, https://developers.google.com/maps/documentation/javascript/maptypes#MapCoordinates, accessed Jul 21th 2015.

[15] Emgu CV, http://www.emgu.com/wiki/index.php/Main_Page, accessed Jul 21th 2015.

[16] OpenCV-Python Tutorials, Morphological Transformations, http://opencv-python-tutroals.readthedocs.org/en/latest/py_tutorials/py_imgproc/py_morphological_ops/py_morphological_ops.html, accessed Jul 21th 2015.

[17] Emgu CV Library Documentation, http://www.emgu.com/wiki/files/2.3.0/document/html/28088b77-7d94-d1a7-9793-8dcec6b70ac5.htm, accessed Jul 21th 2015.